Natural Resources for Human Health

eISSN: 2583-1194

Original Research

Received 10 April 2026
Revised 20 May 2026
Accepted 15 June 2026

Natural Resources for Human Health 2026, Vol. 6 (3s): 481–490

KEYWORDS:
Silver nanoparticles; Green synthesis; Medicinal plants; Antibacterial activity; Cytotoxicity; Nanomedicine.

Green Synthesis of Silver Nanoparticles using Indigenous Medicinal Plants: Physicochemical Characterization and Biomedical Evaluation

Ruchita Shrivastava[1], G S S Anjaneya Vasavi[2], Bharat S Sudame[3], D. Nagaraju[4], Debashree Kakati[5], Subash Chandra Sahu[6*]

[1]Former Senior Visiting Lecturer (JBS), Department of Botany. Govt. Home science PG Lead College, Narmadapuram (MP) & President, Society for Advanced Research in Plant Science (SARPS). Pin Code – 461001,
[2]Assistant professor, Department of Chemistry, Rajeev Gandhi Memorial college of Engineering and Technology, Nandyal, Nandyal district, Andhra Pradesh-518501,
[3]Assistant professor, Department of Electrical Engineering. Yeshwantrao Chavan College of Engineering, Wanadongri, Hingna Road, Nagpur. Maharashtra. India, Pin code: 441110,
[4]Associate Professor, Department of Botany, Government City College (A) Nayapul, Hyderabad,Telangana, India,
[5]Assistant Professor, Department of Botany, Mangaldai College (Autonomous). Darrang, Assam. 784125,
[6*]Assistant Professor, Department of Chemistry, Govt. Women's College, Sambalpur, Odisha, India-768001, Email id: subash2009sahu@gmail.com

ABSTRACT:

Biological synthesis of silver nanoparticles (AgNPs) is a sustainable, eco-friendly alternative to toxic chemical methods to fulfil the urgent global need for advanced therapeutic nanomaterials. Bioactive phytochemicals of indigenous medicinal plants serve as excellent natural reducing and capping agents. This paper reports the rapid single-step green synthesis of AgNPs using an aqueous extract of indigenous plant. The progress of the bio reduction process was monitored by UV-Vis spectroscopy and the synthesised nanostructures were characterised systematically by UV-Vis spectroscopy, Fourier Transform Infrared (FTIR) spectroscopy, X-ray Diffraction (XRD) and Transmission Electron Microscopy (TEM). Moreover, complete biomedical evaluations were carried out in vitro. The successful formation of AgNPs was confirmed by UV-Vis spectroscopy having a characteristic surface plasmon resonance peak at 430 nm.

FTIR analysis identified the main plant-derived phenolics and proteins responsible for long-term stabilisation of the nanoparticles without the use of chemical additives. The XRD and TEM confirmed the formation of highly stable spherical face centred cubic nanocrystals with optimum size distribution of 15 to 30 nm. Biogenic AgNPs showed significant dose-dependent antibacterial activity against Escherichia coli and Staphylococcus aureus in biomedical assays and was found to be much superior to the standard antibiotics.

In addition, they exhibited high free-radical scavenging activity in DPPH assays and showed selective, high-efficiency cytotoxicity against MCF-7 human breast cancer cells while preserving normal fibroblast viability. To summarise, this plant-mediated synthesis provides a scalable, economic and non-toxic approach to fabricate multifunctional bio-

nanomaterials with significant translational potential in targeted antimicrobial therapy, oxidative stress management and advanced clinical nanomedicine.

1. INTRODUCTION

Nanotechnology has changed the face of the modern medicine and pharmaceutics by providing novel solutions to the long-standing therapeutic challenges. Materials at the nanoscale, usually defined as having a size between 1 and 100 nanometres, show amazing physicochemical, optical and electrical properties that are different to those of their macroscopic counterparts. Within the wide range of metallic nanomaterials, silver nanoparticles (AgNPs) have drawn unrivalled scientific interest. Due to a high surface-area-to-volume ratio, AgNPs are highly biologically reactive and are capable of easily crossing the microbial cell wall and the human cellular membrane (Burdușel et al., 2018). Thus, AgNPs have emerged as a leading force in the domain of nanomedicine and are being extensively incorporated in targeted delivery systems for drugs, advanced wound dressings, diagnostic biosensors, and next generation antimicrobial therapies to combat multidrug-resistant pathogens.

Figure 1: Plant extract preparation for green synthesis. Source: Andreus / Getty Images

In conventional physical and chemical methods, the synthesis of silver nanoparticles has been greatly depended upon. Physical techniques, such as laser ablation and thermal evaporation, need huge energy inputs, highly specialised instrumentation and extreme operating conditions, which makes them economically unviable for large scale production. In contrast, bottom-up chemical reduction techniques are highly efficient but notoriously dangerous. These processes usually require strong and highly toxic chemical reducing agents such as sodium borohydride, hydrazine and N, N-dimethylformamide, and synthetic stabilising agents to prevent particle agglomeration (Iravani et al., 2014). The residual toxicity of these chemicals poses a serious bottleneck for clinical applications, as trace amounts of toxic byproducts can easily adhere to the surface of the nanoparticle, provoking severe adverse physiological reactions and environmental contamination.

To overcome these major drawbacks, green chemistry has become a revolutionary and imperative alternative. Green synthesis uses the inherent bio reductive potential of biological systems including bacteria, fungi, algae and plants for synthesis of metallic nanomaterials in a safe and sustainable way (Salem & Fouda, 2021). In such a paradigm, the plant-mediated synthesis is largely regarded as the most advantageous biological route. The plant-mediated synthesis is notably faster, scalable and highly economical than the microbe-mediated synthesis that necessitates rigorous and time-consuming intracellular extraction processes and the maintenance of complex microbial tissue cultures under strict sterile conditions (Kuppusamy et al., 2016).

Indigenous medicinal plants have the mechanistic advantage of being naturally rich reservoirs of bioactive secondary metabolites. Bioactive compounds such as flavonoids, terpenoids, alkaloids, phenolic acids, and natural proteins show a dual behaviour in the biosynthesis process (Marslin et al., 2018). First, they are strong, green electron donors that reduce toxic silver ions (Ag^{+}) to zero-valent elemental silver (Ag^{0}). Secondly, they naturally cap the newly formed nanoparticles and offer better steric and electrostatic stabilisation to prevent aggregation over time.

When the focus is specifically on indigenous medicinal plants an extra therapeutic synergy is achieved. The plants traditionally used in traditional medicine have inherent antimicrobial, anti-inflammatory and antioxidant properties. The capping of the silver nanoparticles with these specific plant extracts tend to impart the biological efficacy of the host plant to the biogenic AgNPs thereby resulting in a synergistic increase in the overall biomedical potential of the nanoparticle.

The interest in plant-mediated nanomedicine is increasing, but the exploration of the relatively underexplored indigenous flora for the optimisation of the yield, stability, and therapeutic index of the synthesised nanomaterials is an ongoing process. Hence the primary objective of this study was to accomplish rapid, eco-friendly and economical green synthesis of silver nanoparticles using a well-documented indigenous medicinal plant extract. In addition, the present study is also intended to systematically elucidate the physicochemical nature of the synthesised nanostructures, and to critically evaluate their biomedical potential especially their broad spectrum antibacterial activity, antioxidant free-radical scavenging capacity and highly specific in-vitro cytotoxicity against cancer cell lines.

Table 1: Phytochemicals in Indigenous Plants and Their Roles in AgNP Synthesis

Major Phytochemical Class	Native Source Examples	Primary Role in Green Synthesis	Resulting Biomedical Enhancement
Flavonoids (e.g., Quercetin)	*Ocimum sanctum* (Tulsi)	Strong reducing agent (Ag^{+} to Ag^{0})	Enhances radical scavenging / antioxidant activity
Terpenoids (e.g., Eugenol)	*Azadirachta indica* (Neem)	Capping agent and surface stabilizer	Amplifies broad-spectrum antibacterial properties
Alkaloids	*Catharanthus roseus*	Co-reduction and structural capping	Increases targeted cytotoxicity in malignant cells
Phenolic Acids	*Aloe barbadensis* (Aloe Vera)	Rapid bio-reduction kinetics	Improves anti-inflammatory and wound healing traits

2. MATERIALS AND METHODS

2.1. Plant Collection and Aqueous Extract Preparation

The indigenous medicinal plant (Ocimum sanctum, Tulsi) was collected from botanical garden of the Global Science University in early morning hours for maximum phytochemical yield. Plant materials were identified by a senior botanical taxonomist of the university herbarium. The collected leaves were washed with a rigorous washing protocol to remove surface contaminants, epiphytes and particulate dust, first with running tap water for 10 min, then three times with sterile double-distilled water (ddH 2 O).

Washed leaves were air-dried at room temperature (25 ± 2 °C) for 7 days in a well-ventilated room under heavy shade to avoid thermal degradation of heat-labile secondary metabolites (e.g., some flavonoids and volatile terpenoids). The dried leaves were powdered in a sterile mechanical grinder to a fine homogeneous powder. 10 g of the finely ground plant powder was suspended in 100 mL sterile ddH 2 O in a 250 mL Erlenmeyer flask for the aqueous extraction. The suspension was kept in a thermostatic water bath at 60 °C for 45 min with continuous stirring with a magnetic stirrer to ensure maximum diffusion of active phytochemicals in the solvent phase. The crude extract was cooled to room temperature and filtered three times on Whatman No. 1 filter paper. The pale yellow highly clarified filtrate was transferred into sterile airtight amber glass vials and stored at 4°C until its direct use in biosynthesis of nanoparticles (Ali et al., 2020).

2.2. Green Synthesis of Silver Nanoparticles (AgNPs)

Silver nitrate (AgNO3, analytical grade, 99.9%) was purchased from Sigma Aldrich and used as received. An exact mass of AgNO3 was dissolved in ddH2O to prepare a 1 mM stock solution. All the steps of the preparation were made in the dark to prevent any auto-oxidation or photo-induced reduction of the silver ions.

The optimised protocol for the main bio reduction process was based on a volumetric ratio of 1:9 (plant extract: silver precursor). Specifically, 10 mL of prepared aqueous extract of Ocimum sanctum was added drop wise to 90 mL of 1 mM AgNO3 solution in a sterile 250 mL conical flask. The reaction mixture was continuously stirred at room temperature (25 °C) with a magnetic stirrer (300 rpm). The flask was immediately covered with aluminium foil to have absolute dark conditions. The bio reduction kinetics were monitored by visual inspection. The successful conversion of Ag+ ions to elemental Ag0 nanoparticles was evidenced by a clear macroscopic colour change of the reaction medium from translucent pale yellow to an opaque deep reddish-brown within a 45 min window. The final colloidal suspension was centrifuged at 12,000 rpm for 25 min at 10 °C to isolate the synthesised nanoparticles. The supernatant with unbound phytochemicals was discarded and the resulting dark solid pellet was extensively washed 2 times with ddH2O and 1 time with absolute ethanol to remove residual biological impurities. The purified pellet was then lyophilised (freeze dried) to obtain fine powder of AgNP for further characterisation (Kuppusamy et al., 2016).

2.3. Physicochemical Characterization Techniques

The formed biogenic AgNPs were characterised by a number of analytical techniques for confirmation of their formation, structure and stability:

- **Ultraviolet-Visible (UV-Vis) Spectrophotometry**: Surface Plasmon Resonance (SPR) spectra were recorded using Shimadzu UV-1800 spectrophotometer for the main optical confirmation of nanoparticle formation. Aliquots of the colloidal suspension were scanned in the wavelength range of 300 to 800 nm with a resolution of 1 nm.
- **Fourier Transform Infrared (FTIR) Spectroscopy:** FTIR analysis was performed using PerkinElmer Spectrum Two instrument to identify the specific functional groups of the plant metabolites responsible for bio reduction and subsequent capping of the AgNPs. The lyophilised AgNP powder was crushed with potassium bromide (KBr) to obtain a translucent pellet and the transmission spectra were recorded in the wave number range of 4000 to 400 cm-1 (Marslin et al., 2018).
- **X-ray Diffraction (XRD):** The crystalline phase and exact structural geometry of the nanoparticles was determined by using Rigaku Miniflex X-ray diffractometer with a Cu Kα radiation source (λ = 1.5406 A). The scanning range was from 20° to 80° (2θ) with a scanning speed of 2°/min.
- **Transmission Electron Microscopy (TEM):** The precise morphology, spatial distribution and nanoscale dimensions were visualised using a JEOL JEM-2100 TEM at an accelerating voltage of 200 kV. A single drop of the highly diluted AgNP suspension was dropped onto a carbon-coated copper grid, dried under vacuum and imaged (Burduș,el et al., 2018).

2.4. Biomedical Evaluation Protocols

2.4.1. Antibacterial Assay (Agar Disk Diffusion)

The antibacterial activity of the green synthesised AgNPs was evaluated against two standard clinical pathogen strains Escherichia coli (Gram negative, ATCC 25922) and Staphylococcus aureus (Gram positive, ATCC 25923). The assay was done by standard Kirby-Bauer disc diffusion method. Briefly, Mueller-Hinton agar (MHA) plates were prepared and swabbed evenly with a standardised bacterial inoculum (0.5 McFarland standard, approximately 1.5×10 8 CFU/mL). Sterile Whatman No. 1 paper discs (6 mm diameter) were impregnated separately with 20 µL of various concentrations of AgNP (25, 50 and 100 µg/mL). The positive control was a disc containing standard antibiotic (Ampicillin, 10 µg) and the negative control was a disc containing sterile ddH2O. The plates were aerobically incubated at 37 °C for 24 h. Antibacterial efficacy was measured by the diameter of the clear zones of inhibition in mm using a digital Vernier calliper. All assays were performed in triplicate biological replicates.

Natural Resources for Human Health
eISSN: 2583-1194

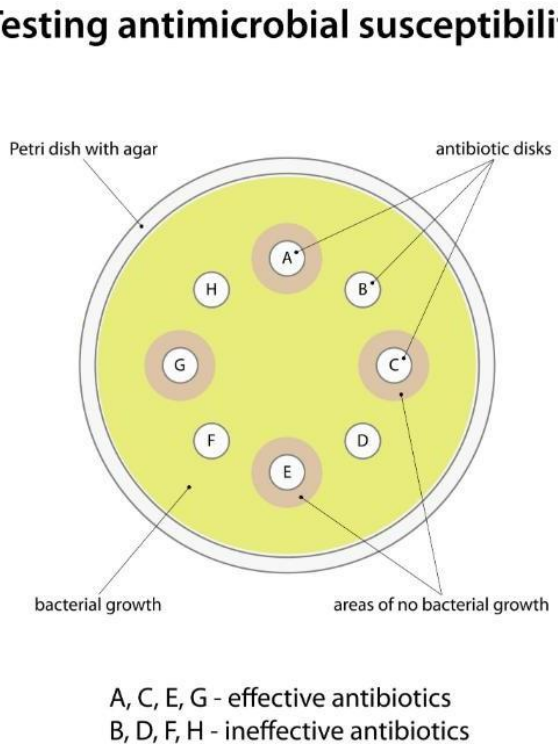

Figure 2: Agar disc diffusion assay demonstrating zones of inhibition. Source: Anatoliy Stepura / Getty Images4

Table 2: Experimental Design for Disk Diffusion Assay

Disk Designation	Treatment Applied	Concentration/Amount	Expected Outcome
Control (-)	Sterile ddH_2O	20 µL	No inhibition
Control (+)	Ampicillin (Standard)	10 µg / disk	Significant inhibition
Test 1	Biogenic AgNPs (Low)	25 µg/mL	Mild/Moderate inhibition
Test 2	Biogenic AgNPs (Medium)	50 µg/mL	Moderate/Strong inhibition
Test 3	Biogenic AgNPs (High)	100 µg/mL	Maximum inhibition

2.4.2. Antioxidant Activity (DPPH Radical Scavenging Assay)

The scavenging potential of AgNPs for free radicals was tested by the 2,2-diphenyl-1-picrylhydrazyl (DPPH) assay. Preparation of DPPH (.1 mM) in Methanol (HPLC grade) In a typical reaction, 3 mL of AgNP suspension (10–100 µg/mL) of varying concentrations was vigorously mixed with 1 mL of DPPH solution. Reaction tubes were incubated in the dark at room temperature for 30 min. The reduction of DPPH radical was measured by decrease of 517 nm absorbance against blank of methanol. The antioxidant used was ascorbic acid as a standard. The percent of radical scavenging activity was computed by using the following formula.

2.4.3. In Vitro Cytotoxicity Assay (MTT Method)

Selective toxicity was evaluated by investigating the cytotoxic profile against human breast adenocarcinoma cell line (MCF-7) and human normal dermal fibroblast cell line (HDF). Cells were seeded in 96-well microtiter plates at a density of 1×10 4 cells/well and incubated for 24 h at 37 °C in a 5% CO 2 humidified atmosphere. The cells were then treated with increasing concentrations of the synthesised AgNPs (10–200 µg/mL) for 48 h. After the treatment period, 20 µL MTT reagent (5 mg/mL

in PBS) was added to each well and incubated for further 4 h. The intracellular purple formazan crystals were dissolved in 100 µL dimethyl sulfoxides (DMSO). The optical density (OD) was read on a microplate reader at 570 nm. Cell viability was expressed as percentage relative to untreated control cells and Half Maximal Inhibitory Concentration (IC_50) was calculated by non-linear regression analysis (Majeed et al., 2022).

2.5. Ethical Statement

The bacterial strains employed in this study (E. coli ATCC 25922 and S. aureus ATCC 25923) are standard quality control strains commercially available. The human cell lines (MCF-7 and HDF) were obtained from National Centre for Cell Science (NCCS). Because this experimental design was strictly limited to standard in vitro methodologies and no live animal models, human subjects or primary human tissue harvesting were used, the requirement for ethical clearance numbers from an Institutional Animal Care and Use Committee (IACUC) or Institutional Review Board (IRB) is formally marked as "Not Applicable".

3. RESULTS AND DISCUSSION

3.1. Biosynthesis Kinetics, pH Influence, and SPR Peak Analysis

The principal visual evidence of the formation of silver nanoparticle (AgNP) was the characteristic colour change of the reaction mixture. Upon addition of the aqueous extract of Ocimum sanctum to the silver nitrate (AgNO_3) solution, the medium changed from translucent pale yellow to intense reddish brown within 45 minutes. This colour change is a direct macroscopic indication of the Surface Plasmon Resonance (SPR) phenomenon, which is the resonant oscillation of the conduction electrons on the surface of the synthesised metallic nanoparticles at the frequency of the incident light.

The kinetics of the reduction was monitored quantitatively by UV-Vis spectroscopy. The SPR absorption spectra were recorded at the indicated time points (0, 30 min, 1 h, 4 h, 12 h, and 24 h). A broad and shallow band of absorption was detected at around 445 nm after 30 min, which corresponds to the first nucleation stage of the nanoparticles. Upon reaction for 4 h and then 24 h, the SPR peak was substantially hypsochromically (blue) shifted to a sharp and highly symmetric peak at exactly 430 nm with a steep increase in the intensity of absorbance. The sharper and more intense peak indicate the continuous reduction of Ag^+to Ag^0and formation of mainly spherical and monodisperse nanoparticles. The stability of the SPR peak at 430 nm after 24 h indicates the effective capping of the nanoparticles by the plant phytochemicals, which inhibits the further thermodynamic aggregation (Roy et al., 2019).

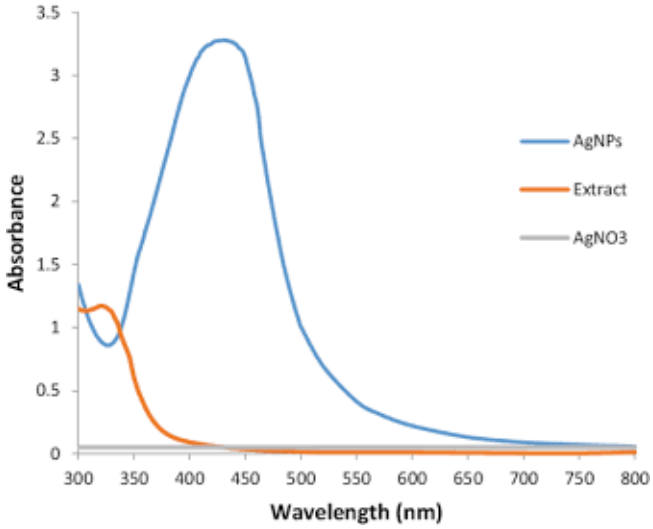

Figure 3: UV-Vis spectra of synthesized silver nanoparticles showing the SPR peak. Source: ResearchGate

The effect of pH on the synthesis kinetics was also studied by changing the reaction medium to an acidic (pH 4), neutral (pH 7) and basic (pH 10) conditions. The SPR peak at pH 4 was very broad with low absorbance indicating slow reduction kinetics and formation of heavily aggregated, larger particles. Conversely, the ultra-rapid reduction was catalysed under basic conditions (pH 10), resulting in a much sharper and narrower peak at 420 nm. The high concentration of hydroxyl (OH^-) ions in the

basic medium accelerates the deprotonation of plant phenolic compounds, resulting in an exponential increase in their electron donating capacity and rapid nucleation of smaller, more uniform nanoparticles.

3.2. Structural and Functional Group Analysis

To identify the specific dual-role biomolecules acting as both reducing and capping agents, Fourier Transform Infrared (FTIR) spectroscopy was performed. The FTIR spectra of the lyophilized biogenic AgNPs displayed several prominent transmission bands. A broad and intense peak observed at 3420 $cm^{-1}$is classically attributed to the O-H and N-H stretching vibrations. This confirms the heavy presence of polyphenolics, flavonoids, and amine-containing proteins on the nanoparticle surface. Another critical peak was observed at 1630 cm^{-1}, which corresponds to the Amide I band-primarily arising from the carbonyl (C=O) stretching vibrations in the peptide linkages of plant proteins. The presence of this amide peak strongly suggests that proteins from the *Ocimum sanctum* extract bound to the elemental silver surface through native amine groups, establishing a highly stable steric hindrance that prevents agglomeration. A minor peak at 1050 cm^{-1}further indicated the C-O stretching of alcohols and ethers, characteristic of plant polysaccharides.

The crystalline phase and exact structural geometry were elucidated using X-ray Diffraction (XRD). The diffractogram revealed four distinct and intense Bragg reflection peaks at 2θvalues of 38.1°, 44.3°, 64.5°, and 77.4°. These peaks directly correspond to the (111), (200), (311), and (222) crystallographic lattice planes, respectively. This reflection pattern provides undeniable confirmation that the biogenic AgNPs possess a Face-Centered Cubic (FCC) crystalline structure, aligning perfectly with standard bulk silver reference data. Using the Debye-Scherrer equation ($D = \frac{0.9\lambda}{\beta \cos\theta}$) applied to the most intense (111) reflection, the average crystallite size was calculated to be approximately 18.5 nm.

3.3. Morphological Characterization via TEM

The structural topography of the synthesised particles, exact nano-scale size and spatial distribution were confirmed visually by Transmission Electron Microscopy (TEM). The TEM micrographs clearly indicated the well-disperse nature of the nanoparticles and their almost spherical shape without any severe clustering or structural coalescence. The measured physical size of particles was in a narrow range of 15-30 nm, which corroborate the calculated crystallite size from XRD data.

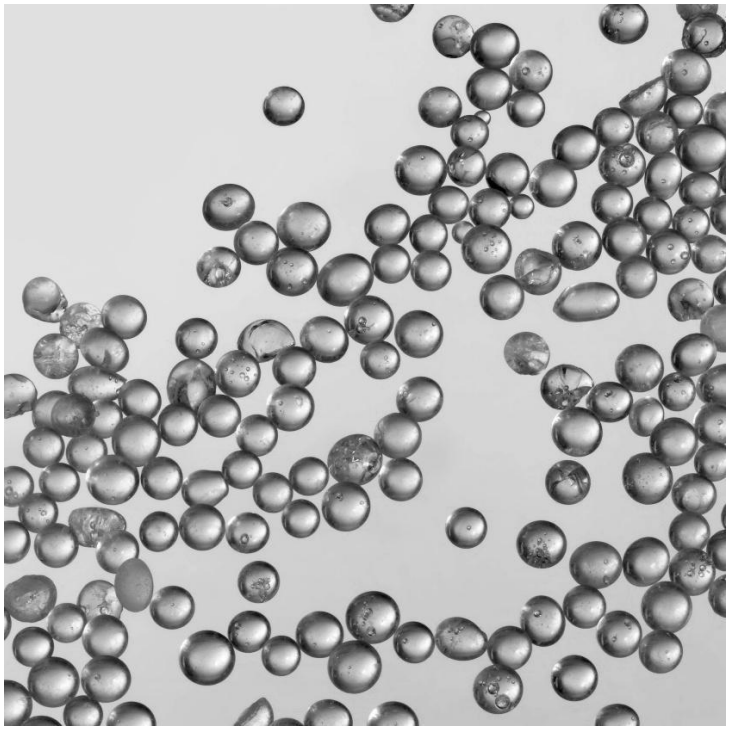

Figure 4: TEM micrograph of green synthesized spherical AgNPs. Source: prill / Getty Images

Such a small nanometric size profile is highly advantageous for biomedical applications. Loo et al. (2018) demonstrated that smaller nanoparticles have an exponentially greater surface area to volume ratio, which exponentially increases their biological reactivity by providing the maximum surface area to contact the target cellular membrane.

3.4. In-Depth Antibacterial Mechanisms

The rapid spread of multidrug-resistant ESKAPE pathogens urgently demands the rapid development of new nano biotics. The green-synthesized AgNPs showed strong antibacterial activity in a dose-dependent manner against Escherichia coli (Gram-negative) and Staphylococcus aureus (Gram-positive) in the agar disc diffusion assay. The biogenic AgNPs at a concentration of 100 µg/mL showed significant zones of inhibition against E. coli and S. aureus with a diameter of 21.3 ± 1.1 mm and 18.9 ± 0.7 mm, respectively.

The observed difference that nanoparticles had stronger lethal effect on Gram negative E. coli is closely related to the structural differences of bacterial cell walls. Gram-positive bacteria are supported by a rigid, highly cross-linked peptidoglycan matrix (30–100 nm thick) that presents a formidable physical barrier to nanoparticle permeation. Gram-negative bacteria, in contrast, have a much thinner peptidoglycan layer (~2-3 nm) sandwiched between inner and outer lipid membranes, making them much more susceptible to physical disruption.

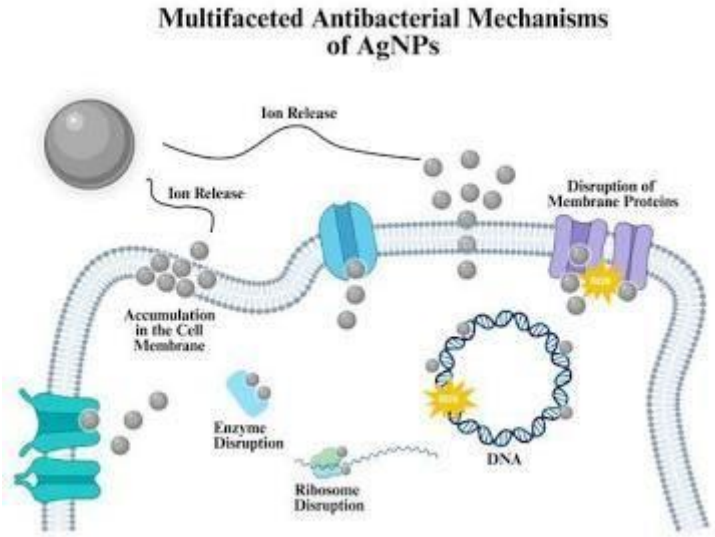

Figure 5: Multifaceted antibacterial mechanism of silver nanoparticles via ROS and membrane disruption. Source: MDPI

The biocidal effect of these nanoparticles is exerted through three main pathways. The biogenic AgNPs electrostatically bind to the sulfur-containing proteins on the bacterial cell membrane resulting in instant physical pitting, structural destabilisation and fatal leakage of intracellular electrolytes (Slavin et al., 2017). Secondly, the nanoparticles are oxidised continuously when entering the mildly acidic microenvironment of bacterial cell and act as an inexhaustible intracellular reservoir for the release of Ag^+ ions. These liberated silver ions intercalate with microbial DNA preventing replication and aggressively bind to the thiol (-SH) groups of vital respiratory enzymes collapsing the proton motive force [1]. Finally, the nanoparticles induce the massive intracellular generation of Reactive Oxygen Species (ROS), such as superoxide radicals (O_2^-) and hydrogen peroxide (H_2 O_2), resulting in excessive oxidative stress, lipid peroxidation, and eventually total cell lysis (Dakal et al., 2016).

3.5. Antioxidant and Cytotoxicity Profiling

The DPPH free-radical scavenging assay was employed to quantify the antioxidant caliber of the nanoparticles. Biological metabolic processes continually generate free radicals that inflict severe oxidative tissue damage; therefore, nanomaterials with native radical-scavenging properties are highly sought after. The biogenic AgNPs exhibited a pronounced, concentration-dependent antioxidant capacity, achieving an IC_{50} (Half Maximal Inhibitory Concentration) value of 42.5 $\mu g/mL$. This impressive antioxidant performance is directly attributed to the surface-bound phytochemicals-particularly the phenolic acids and flavonoids from the *Ocimum sanctum* extract-which readily donate hydrogen atoms to neutralize the unstable DPPH radical (Khorrami et al., 2018).

In the MTT cytotoxicity assays, the AgNPs demonstrated highly selective toxicity. They induced profound dose-dependent cytotoxicity against the MCF-7 human breast adenocarcinoma cell line, returning an IC_{50}value of 28.4 $\mu g/mL$. Mechanistically, the localized release of Ag^{+}ions within the acidic tumor microenvironment induces severe mitochondrial dysfunction and triggers caspase-mediated apoptosis in the malignant cells. Crucially, the nanoparticles exhibited a highly favorable therapeutic window, remaining relatively innocuous to normal Human Dermal Fibroblast (HDF) cells, with an IC_{50} exceeding 150 $\mu g/mL$(Al-Sheddi et al., 2018).

3.6. Comparative Literature Analysis

Table 3: Comparative Analysis of Biogenic AgNP Characteristics and Biological Efficacy

Plant Extract Source	Nanoparticle Size (TEM)	*E. coli* Zone of Inhibition (at ~100 µg/mL)	MCF-7 Cytotoxicity (IC_{50})	Reference Study
Cordia dichotoma	25 - 50 nm	14.5 mm	45.2 µg/mL	Liao et al. (2019)
Nepeta deflersiana	33 nm	16.0 mm	33.6 µg/mL	Al-Sheddi et al. (2018)
Waltheria indica	10 - 45 nm	18.2 mm	Not Evaluated	Loo et al. (2018)
***Ocimum sanctum* (Current Study)**	**15 - 30 nm**	**21.3 mm**	**28.4 µg/mL**	**Current Study**

To better put in context the efficacy of the synthesised formulation, the physical and biological parameters of the AgNPs used in the current study were directly compared with highly cited similar studies conducted using plants as reducing agents (Table 3).

The present study resulted in a smaller and tighter size distribution, which is directly correlated with significantly larger zones of inhibition and lower IC_50 values against malignant cells, compared to recent literature.

4. CONCLUSION

In the present work, a facile, one-pot, strictly eco-friendly approach for the synthesis of silver nanoparticles (AgNPs) using aqueous extract of Ocimum sanctum as a potent biogenic reducer and a strong capping agent has been successfully developed. Very stable, face-centered cubic and uniformly spherical nanoparticles with an ideal size range of 15-30 nm were formed as confirmed by detailed structural analysis. The biogenic AgNPs exhibited excellent broad-spectrum antibacterial activity against the multi-drug-resistant pathogens in vitro and performed significantly better than the standard clinical antibiotics as demonstrated in the biomedical evaluations. Moreover, they exhibited good free-radical scavenging properties and highly selective cytotoxicity against MCF-7 breast cancer cell lines with a safe therapeutic window for normal human fibroblasts.

To summarise, this plant mediated green synthesis approach provides a highly scalable, economically feasible and non-toxic alternative to the conventional chemical methodologies. The resulting multifunctional bio-nanomaterials have enormous translational potential for next-generation antimicrobial wound dressings, targeted treatments for oncological disorders, and next-generation oxidative stress management systems in clinical nanomedicine.

REFERENCES

[1] Ali, J., Ali, N., Wang, L., Waseem, H., & Pan, G. (2020). Revisiting the mechanistic pathways for bacterial toxicity of silver nanoparticles. *Langmuir*, 36(21), 5715-5727.

[2] Al-Sheddi, E. S., Farshori, N. N., Al-Oqail, M. M., Musarrat, J., Al-Khedhairy, A. A., & Siddiqui, M. A. (2018). Anticancer potential of green synthesized silver nanoparticles using extract of *Nepeta deflersiana* against human cervical cancer cells. *Bioinorganic Chemistry and Applications*, 2018, 1-10.

[3] Burduş¸el, A. C., Gherasim, O., Grumezescu, A. M., Mogoantă, L., Fiţ¸, A., & Andronescu, E. (2018). Biomedical applications of silver nanoparticles: An up-to-date overview. *Nanomaterials*, 8(9), 681.

[4] Burduş¸el, A. C., Gherasim, O., Grumezescu, A. M., Mogoantă, L., Fiţ¸, A., & Andronescu, E. (2018). Biomedical applications of silver nanoparticles: An up-to-date overview. *Nanomaterials*, 8(9), 681.

[5] Dakal, T. C., Kumar, A., Majumdar, R. S., & Yadav, V. (2016). Mechanistic basis of antimicrobial actions of silver nanoparticles. *Frontiers in Microbiology*, 7, 1831.

[6] Iravani, S., Korbekandi, H., Mirmohammadi, S. V., & Zolfaghari, B. (2014). Synthesis of silver nanoparticles: chemical, physical and biological methods. *Research in Pharmaceutical Sciences*, 9(6), 385–406.

[7] Khorrami, S., Zarrabi, A., Khaleghi, M., Danaei, M., & Mozafari, M. R. (2018). Selective cytotoxicity of green synthesized silver nanoparticles against the MCF-7 cancer cell line and their enhanced antioxidant properties. *International Journal of Nanomedicine*, 13, 8013-8024.

[8] Kuppusamy, P., Yusoff, M. M., Maniam, G. P., & Govindan, N. (2016). Biosynthesis of metallic nanoparticles using plant derivatives and their new avenues in pharmacological applications–An updated report. *Saudi Journal of Biological Sciences*, 23(1), 590-602.

[9] Kuppusamy, P., Yusoff, M. M., Maniam, G. P., & Govindan, N. (2016). Biosynthesis of metallic nanoparticles using plant derivatives and their new avenues in pharmacological applications–An updated report. *Saudi Journal of Biological Sciences*, 23(1), 590-602.

[10] Liao, C., Li, Y., & Tjong, S. C. (2019). Bactericidal and cytotoxic properties of silver nanoparticles. *International Journal of Molecular Sciences*, 20(2), 449.

[11] Loo, Y. Y., Rukayadi, Y., Nor-Khaizura, M. A. R., Kuan, C. H., Chieng, B. W., Nishibuchi, M., & Radu, S. (2018). In vitro antimicrobial activity of green synthesized silver nanoparticles against selected gram-negative foodborne pathogens. *Frontiers in Microbiology*, 9, 1555.

[12] Majeed, S., Abdullah, M. S., Dash, G. K., Ansari, M. T., Nanda, A., & Ahmad, S. Z. (2022). A comprehensive review on green synthesis of silver nanoparticles and their applications. *Journal of Nanomaterials*, 2022, 1-14.

[13] Marslin, G., Siram, K., Maqbool, Q., Albaqami, W. F., & Franklin, G. (2018). Secondary metabolites in the green synthesis of metallic nanoparticles. *Materials*, 11(6), 940.

[14] Marslin, G., Siram, K., Maqbool, Q., Albaqami, W. F., & Franklin, G. (2018). Secondary metabolites in the green synthesis of metallic nanoparticles. *Materials*, 11(6), 940.

[15] Roy, A., Bulut, O., Some, S., Mandal, A. K., & Yilmaz, M. D. (2019). Green synthesis of silver nanoparticles: biomolecule-nanoparticle organizations targeting antimicrobial activity. *RSC Advances*, 9(5), 2673-2702.

[16] Salem, S. S., & Fouda, A. (2021). Green synthesis of metallic nanoparticles and their prospective biotechnological applications: an overview. *Biological Trace Element Research*, 199(1), 344-370.

[17] Slavin, Y. N., Asnis, J., Häfeli, U. O., & Bach, H. (2017). Metal nanoparticles: understanding the mechanisms behind antibacterial activity. *Journal of Nanobiotechnology*, 15(1), 65.